Development 133, 1219-1229 (2006) doi:10.1242/dev.02298

Multiple roles of mesenchymal β-catenin during murine limb patterning

Theo P. Hill[1], Makoto M. Taketo[2], Walter Birchmeier[3] and Christine Hartmann[1,*]

Recently canonical Wnt signaling in the ectoderm has been shown to be required for maintenance of the apical ectodermal ridge (AER) and for dorsoventral signaling. Using conditional gain- and loss-of-function β-catenin alleles, we have studied the role of mesenchymal β-catenin activity during limb development. Here, we show that loss of β-catenin results in limb truncations due to a defect in AER maintenance. Stabilization of β-catenin also results in truncated limbs, caused by a premature regression of the AER. Concomitantly, in these limbs, the expression of *Bmp2*, *Bmp4* and *Bmp7*, and of the Bmp target genes *Msx1*, *Msx2* and gremlin, is expanded in the mesenchyme. Furthermore, we found that the expression of *Lmx1b*, a gene exclusively expressed in the dorsal limb mesenchyme and involved in dorsoventral patterning, is reduced upon loss of β-catenin activity and is expanded ventrally in gain-of-function limbs. However, the known ectodermal regulators *Wnt7a* and engrailed 1 are expressed normally. This suggests that *Lmx1b* is also regulated, in part, by a β-catenin-mediated Wnt signal, independent of the non-canoncial Wnt7a signaling pathway. In addition, loss of β-catenin results in a severe agenesis of the scapula. Concurrently, the expression of two genes, *Pax1* and *Emx2*, which have been implicated in scapula development, is lost in β-catenin loss-of-function limbs; however, only *Emx2* is upregulated in gain-of-function limbs. Mesenchymal β-catenin activity is therefore required for AER maintenance, and for normal expression of *Lmx1b* and *Emx2*.

KEY WORDS: β-Catenin, Limb patterning, Scapula, *Emx2*, AER, *Lmx1b*, BMP, Dorsoventral axis

INTRODUCTION

The complex structure of the vertebrate limb requires the correct formation of early signaling centers that define the primary axes of the early limb bud and the subsequent patterning of internal structures such as skeletal elements (Tickle, 2003). Members of the Wingless/Int (Wnt) family of secreted signaling molecules have been shown to play important roles in both of these processes (Church et al., 2002; Yang, 2003). In chick, *Wnt2b* and *Wnt8c* have been implicated in *Fgf10* activation via the canonical Wnt/β-catenin pathway, thereby inducing limb bud outgrowth (Kawakami et al., 2001; Ng et al., 2002). *Fgf10* in the mesenchyme is required for induction of the apical ectodermal ridge (AER) marker *Fgf8* in a strip of flank ectoderm before the formation of a morphological AER (Martin, 1998). The AER is a strip of stratified epithelia at the distal limb bud margin that is essential for limb outgrowth and for proximodistal patterning (Saunders, 1948). Induction of *Fgf8* by mesenchymal *Fgf10* is thought to be mediated by ectodermal Wnt signals, such as *Wnt3a* in chick and *Wnt3* in mouse, which activate and maintain the expression of *Fgf8* in the AER through the canonical Wnt/β-catenin pathway (Barrow et al., 2003; Kengaku et al., 1998; Soshnikova et al., 2003). At least two of the β-catenin co-factor genes, lymphoid enhancer binding factor 1 (*Lef1*) and T-cell factor 1 (*Tcf1*; *Tcf7* – Mouse Genome Informatics), are required for *Fgf8* expression in mice (Galceran et al., 1999). However, in *Lef1/Tcf1* double-mutant mice, *Fgf10* expression is initiated normally, which might be due to residual canonical Wnt signaling, as two other members of the Tcf family, *Tcf3* and *Tcf4* (*Tcf7l2* – Mouse Genome Informatics), are still present (Agarwal et al., 2003). Signals from the AER are involved in two important feedback loops, one with the distal mesenchyme required for AER maintenance and further outgrowth of the limb; the other one with the zone of polarizing activity (ZPA), which is important for AER regression (Niswander, 2003; Tickle, 2003). In the latter, *Fgf4*, probably together with other Fgfs, maintains the expression of *Shh* in the ZPA (Chiang et al., 1996; Laufer et al., 1994). *Shh* in turn downregulates Bmp activity by directly or indirectly inducing the Bmp-antagonist gremlin (*Grem1* – Mouse Genome Informatics) (Khokha et al., 2003). Without gremlin, the AER regresses prematurely as a result of the downregulation of *Fgf4* (and probably *Fgf9* and *Fgf17*) by Bmps in the posterior AER (Guha et al., 2002; Khokha et al., 2003; Pizette and Niswander, 1999; Zuniga et al., 1999; Zuniga et al., 2004). During normal limb development, this feedback loop stops, leading to regression of the AER when regions of the limb mesenchyme can no longer respond to *Shh* and, thus, gremlin becomes downregulated (Scherz et al., 2004).

In addition, Wnt signaling is required for dorsoventral patterning of the limb mesenchyme. *Wnt7a* is expressed only in the dorsal ectoderm because of the activity of the ventral ectodermally expressed engrailed 1 (*En1*) (Loomis et al., 1996; Parr and McMahon, 1995). *Wnt7a* regulates expression of the transcription factor *Lmx1b*, known as *Lmx1* in chick, presumably through a non-canonical signaling pathway (Cygan et al., 1997; Kengaku et al., 1998; Riddle et al., 1995; Vogel et al., 1995). *Lmx1b*, expressed exclusively in the dorsal mesenchyme, is required for the specification of dorsal limb identity in mouse and chick (Chen et al., 1998; Dreyer et al., 1998; Riddle et al., 1995; Vogel et al., 1995).

Previous loss-of-function studies in mouse addressing the role of canonical Wnt-signaling in limb patterning either solely focused on its role in the ectoderm, or did not allow the differences between the mesenchymal and the ectodermal contribution to be distinguished (Barrow et al., 2003; Galceran et al., 1999; Soshnikova et al., 2003). Therefore, we specifically addressed the contribution of

[1]Research Institute of Molecular Pathology (IMP), Dr Bohr-Gasse 7, A-1030 Vienna, Austria. [2]Department of Pharmacology, Graduate School of Medicine, Kyoto University, Yoshida-Konoe-cho, Sakyo-ku, Kyoto 606-8501, Japan. [3]Max Delbrück Center for Molecular Medicine, Robert-Roessle-Strasse 10, 13125 Berlin, Germany.

*Author for correspondence (e-mail: hartmann@imp.univie.ac.at)

Accepted 24 January 2006

mesenchymal β-catenin during early limb development using conditional loss- and gain-of-function alleles and the limb mesenchyme-specific Prx1-Cre line. Here, we show that canonical Wnt signaling in the mesenchyme is required for maintaining *Fgf10* and *Fgf8* expression, which suggests a specific role for mesenchymal β-catenin in AER maintenance, in addition to the one proposed in the ectoderm (Barrow et al., 2003; Soshnikova et al., 2003). Interestingly, we also identified a novel role for active Wnt signaling in AER regression. This effect is concomitant with an upregulation of Bmps and Bmp target gene expression, suggesting that canonical Wnt signaling lies upstream of Bmps in the limb mesenchyme.

Unexpectedly, we found that mesenchymal β-catenin is involved in regulating the dorsal determinant *Lmx1b*. Loss of β-catenin activity results in a reduced and partial loss of *Lmx1b* expression, whereas expression of a dominant-active form results in its expansion; however, *Wnt7a* and *En1* remain correctly localized in the dorsal and ventral ectoderm, respectively.

Finally, we found that, unlike many other mutants that affect limb bud outgrowth, loss of mesenchymal β-catenin results in agenesis of the scapula, despite the presence of a humeral-like element. This phenotype is probably primarily due to the loss of expression of the homeobox gene *Emx2* in β-catenin mutant limbs, as *Emx2* mutants also display severe scapula agenesis (Pellegrini et al., 2001). *Emx2* is upregulated in the gain-of-function limbs and is therefore likely to be under the direct control of canonical Wnt signaling.

MATERIALS AND METHODS

Embryo preparation and alkaline phosphatase staining

β-catenin loss-of-function embryos were generated by crossing *Prx1Cre/+;β-cat*$^{+/-}$ males, heterozygous for the β-catenin *lacZ* knock-in allele (–) (Huelsken et al., 2000), to females homozygous for a floxed allele (fl) (Huelsken et al., 2001), to generate *Prx1Cre/+;β-cat*$^{fl/-}$ embryos [hereafter called *β-cat*$^{\Delta Prx1/-}$ or loss of function (lof)]. Gain-of-function embryos were generated by mating female mice homozygous for the β-catenin exon3 floxed allele (ex3fl) (Harada et al., 1999) to *Prx1Cre* heterozygous males to produce *Prx1Cre/+;β-cat*$^{ex3fl/+}$ embryos [hereafter called *β-cat*$^{ex3Prx1/+}$ or gain-of-function (gof)]. *Prx1-Cre* line activity was analyzed by crossing males to Z/AP reporter females (Lobe et al., 1999). Mouse embryos were collected and staged either by counting somites or according to Theiler (Theiler, 1989). Genotypes of the embryos were determined by PCR and by morphology. Embryos were fixed in 4% paraformaldehyde/PBS at 4°C overnight, washed, and dehydrated into either 100% methanol for whole-mount in situ hybridization or 100% ethanol for paraffin wax embedding. Paraffin sections were cut at 5 μm. Whole-mount alkaline phosphatase staining was performed as described previously (Lobe et al., 1999).

Skeletal preparations and scanning electron microscopy (SEM)

Embryos were skinned, eviscerated and fixed in 95% ethanol. Skeletons were stained with Alizarin Red and Alcian Blue, or just with Alcian Blue (McLeod, 1980). For SEM analysis embryos were fixed overnight in 2% glutaraldehyde/0.1 M sodium cacodylate buffer (SCB), pH 7.2, washed in SCB, postfixed for 90 minutes in 1% osmium tetroxide, washed in SCB, and dehydrated into 100% ethanol and critical-point dried.

Whole-mount, section and double-fluorescent in situ hybridisation

Whole-mount and section in situ hybridisation was performed as described previously (Murtaugh et al., 1999; Riddle et al., 1993). For sectioning of whole-mount, stained embryos, embryos were embedded in gelatin and vibratome sectioned at 20 μm. Double-fluorescent in situ hybridisations on paraffin sections were performed using biotin- and DIG-labelled probes. After hybridisation, slides were washed, quenched and blocked. Probes were detected by incubation with streptavidine-HRP (Perkin Elmer, diluted 1 in 100) and anti-DIG-HRP (Roche, diluted 1 in 50), followed by Cy3- or Cy5-tyramide-labelled fluorescent dyes (according to instructions of the TSA Plus Fluorescent Systems kit, Perkin Elmer). All probes have been described previously. The minimum number of specimens analyzed for each marker was three for all stages, except for AER measurements (see legend to Fig. 3), and two for SEM, unless otherwise stated. All comparative images are at the same magnification, unless otherwise noted. AER measurements were performed on *Fgf8*-stained limbs by measuring the pixel number for each limb using Metamorph.

Immunohistochemistry and TUNEL assay

Immunohistochemistry was performed on paraffin sections using monoclonal mouse anti-β-catenin (BD Transduction Laboratories, diluted 1 in 200) after heat-induced antigene retrieval. The signal was detected using a biotinylated secondary antibody (diluted 1 in 250; Vector Laboratories) in combination with the ABC Kit (Vector Laboratories) and DAB substrate (Sigma). TUNEL assays were performed using the Flourescein In Situ Cell Death Kit (Roche).

Micromass cultures

Micromass cultures were performed as described previously (Hill et al., 2005). Primer sequences for RT-PCR are available upon request. Total RNA (1 μg), isolated using TRIZOL from cultures 12 hours and 14 hours after plating and infection, was used for reverse transcription. Semi-quantitative RT-PCR was performed using fivefold dilutions of the cDNA template, starting at a 1 in 10 dilution.

RESULTS

Loss and overactivation of β-catenin in the limb mesenchyme cause limb truncations

In order to address the role of canonical Wnt signaling in the mesenchyme during limb development, we analysed conditional β-catenin loss- and gain-of-function embryos using the mesoderm-specific *Prx1Cre* line (Logan et al., 2002). Loss-of-function *β-cat*$^{\Delta Prx1/-}$ embryos (Fig. 1B) died shortly after birth and had severely shortened fore- and hindlimbs, with respect to wild type (Fig. 1A). Notably, hindlimbs developed further than forelimbs, as can be seen

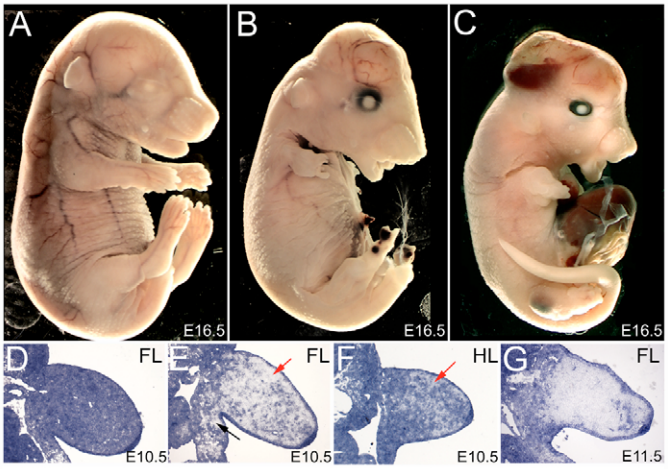

Fig. 1. Loss- and gain-of β-catenin activity in limb mesenchyme causes truncations of the limbs. (**A-C**) Normal wild-type limbs (A), and limb truncations in lof *β-cat*$^{\Delta Prx1/-}$ (B) and gof *β-cat*$^{\Delta ex3Prx1/+}$ (C) E16.5 embryos. (**D-G**) In situ hybridization for β-catenin using the mβ-catenin-del probe. (D) Strong ubiquitous expression in flank and limb mesenchyme, and in the ectoderm and AER of wild-type E10.5 limbs. (E) Loss of β-catenin expression at E10.5 in flank (black arrow) and forelimb (red arrow) mesenchyme in *β-cat*$^{\Delta Prx1/-}$ embryos. (F) Less deletion is detected in E10.5 *β-cat*$^{\Delta Prx1/-}$ hindlimbs (HL, red arrow). (G) Near complete loss of β-catenin expression in the mesenchyme of *β-cat*$^{\Delta Prx1/-}$ E11.5 forelimbs, while ectodermal expression remains normal.

in skeletal preparations at E13.5 and E14.5 (see Fig. S1 in the supplementary material). Gain-of-function *β-cat*$^{\Delta ex3Prx1/+}$ embryos also had shortened limbs (Fig. 1C). Similar to *β-cat*$^{\Delta Prx1/-}$ embryos, forelimbs were more severely affected than hindlimbs (Fig. 1C). From E13.5 onwards, formation of haematomes in distal regions could be observed, primarily but not exclusively, in the hindlimbs of both mutants.

Deletion of β-catenin in the limb ectoderm has been shown to result in patterning defects (Barrow et al., 2003; Soshnikova et al., 2003). Therefore, we confirmed, by in situ hybridization using an antisense probe specific to the floxed exons (*mβ-catenin* del), that β-catenin was still expressed in the ectoderm and the AER in *β-cat*$^{\Delta Prx1/-}$ limbs (Fig. 1E-G). Although wild-type limbs displayed uniform β-catenin expression at E10.5 (Fig. 1D), *β-cat*$^{\Delta Prx1/-}$ forelimbs showed a high degree of deletion in the limb and flank mesenchyme at E10.5 (Fig. 1E, red and black arrow, respectively), and almost complete deletion at E11.5 (Fig. 1G). By contrast, only patchy deletion was detected in the hindlimb mesenchyme at E10.5 (Fig. 1F, red arrow). As has been previously published, by E11.5 deletion had occurred in most mesenchymal cells of the hindlimb (Hill et al., 2005). ZAP-reporter analysis of the Prx1-Cre line revealed that deletion in the forelimb occurred in a mosaic pattern as early as somite stage 15 (see Fig. S2B,B′ in the supplementary material). The different kinetics of deletion observed between fore- and hindlimb (Fig. 1E-G) (see also Logan et al., 2002), are probably responsible for the differences in fore- and hindlimb development of the mutants.

AER defects upon loss of mesenchymal β-catenin activity

Loss of β-catenin in the mesenchyme resulted in severely shortened fore- and hindlimbs. Scanning electron microscopy (SEM) analyses of the forelimbs revealed that the *β-cat*$^{\Delta Prx1/-}$ limb bud was slightly smaller along the anteroposterior (AP) axis at E9.5 (Fig. 2A,A′). At E10.5, *β-cat*$^{\Delta Prx1/-}$ limbs were growth retarded and showed notches in the AER (Fig. 2B,B′). Although we did not observe any gross morphological difference at E9.5, it is possible that molecular changes contributing to the later phenotype have occurred. We therefore analyzed the expression of genes involved in limb outgrowth. *Fgf8*, one of the earliest known ectodermal markers for limb outgrowth, was expressed in its normal stripe-like pattern at 17 somites, before any apparent limb outgrowth had occurred, in wild-type and *β-cat*$^{\Delta Prx1/-}$ limbs (Fig. 2C,C′). At 20 somites, *Fgf8* expression was still comparable in *β-cat*$^{\Delta Prx1/-}$ and wild-type limbs (Fig. 2D,D′). However, at 25 somites, before the morphological appearance of an AER, *Fgf8* expression was reduced in a patchy manner in *β-cat*$^{\Delta Prx1/-}$ limbs (see arrows in Fig. 2E,E′). Shortly after the formation of the stratified AER at stage E10.5, *Fgf8* expression was restricted to patches along the distal margin in *β-cat*$^{\Delta Prx1/-}$ limbs (Fig. 2F,F′). The patchy downregulation of *Fgf8* in the AER and the subsequent loss of the AER suggest a defect in AER maintenance upon loss of β-catenin activity in the mesenchyme.

β-catenin had been implicated in the regulation of *Tbx5* in chick (Kawakami et al., 2001) and *Fgf10* in mouse (Agarwal et al., 2003) during limb bud initiation. We therefore examined their expression in *β-cat*$^{\Delta Prx1/-}$ limbs. Around 19-20 somites, the expression of *Tbx5* and *Fgf10* in *β-cat*$^{\Delta Prx1/-}$ forelimbs was not altered (Fig. 2G,G′,I,I′), suggesting either that these genes are not directly controlled by β-catenin or that the Prx1-Cre line does not delete early and broadly enough to see an effect. However, at E10.75, *Fgf10* expression was downregulated (Fig. 2H,H′), although *Tbx5* expression was still maintained (Fig. 2J,J′, see also Fig. S3A-A″ in the supplementary material).

Overactivation of β-catenin in the limb mesenchyme causes premature AER regression

Because *Fgf8* expression and functional AER activity was significantly affected in forelimbs lacking β-catenin, we analysed whether a gain of mesenchymal β-catenin activity would result in

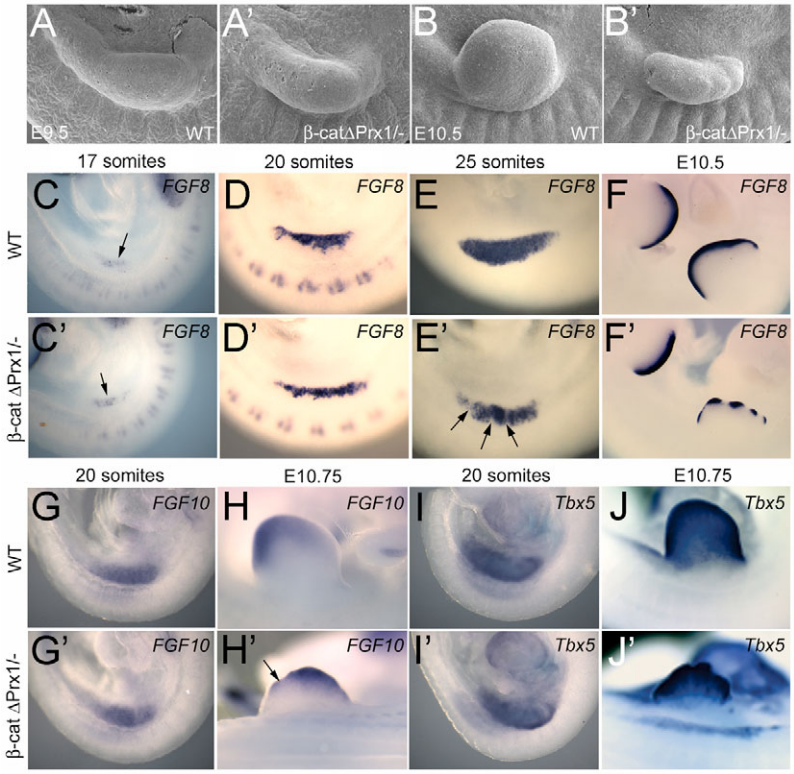

Fig. 2. SEM and marker analysis of limb bud development in *β-cat*$^{\Delta Prx1/-}$ embryos. (**A-B′**) Scanning electron microscopy (SEM) images of wild-type (WT, A,B) and *β-cat*$^{\Delta Prx1/-}$ (A′,B′) forelimbs at E9.5 (A,A′) and E10.5 (B,B′). (**C-E′**) Analysis of *Fgf8* expression in somite staged embryos. *Fgf8* expression (arrow) in a narrow stripe along the body wall at 17 somites in wild type (C) and *β-cat*$^{\Delta Prx1/-}$ (C′). *Fgf8* expression domain at 20 somites in wild type (D) and *β-cat*$^{\Delta Prx1/-}$ (D′). Extensive *Fgf8* expression in wild type (E) at 25 somites, which is reduced in *β-cat*$^{\Delta Prx1/-}$ forelimbs (arrows in E′). (**F**,**F′**) At E10.5, *Fgf8* expression in wild type becomes refined to the AER (F); a dashed expression domain is observed in *β-cat*$^{\Delta Prx1/-}$ forelimbs, corresponding to notches in the AER (F′). (**G**,**G′**) At 19-20 somites, similar *Fgf10* expression is seen in wild type (G) and *β-cat*$^{\Delta Prx1/-}$ (G′) forelimbs. (**H**,**H′**) At E10.75, *Fgf10* expression in the distal mesenchyme is reduced in *β-cat*$^{\Delta Prx1/-}$ forelimbs (arrow, H′) compared with wild type (H). (**I-J′**) *Tbx5* expression at 19-20 somites and at E10.75, comparing wild-type (I,J) and *β-cat*$^{\Delta Prx1/-}$ (I′,J′) forelimbs. Embryos are oriented anterior to the right.

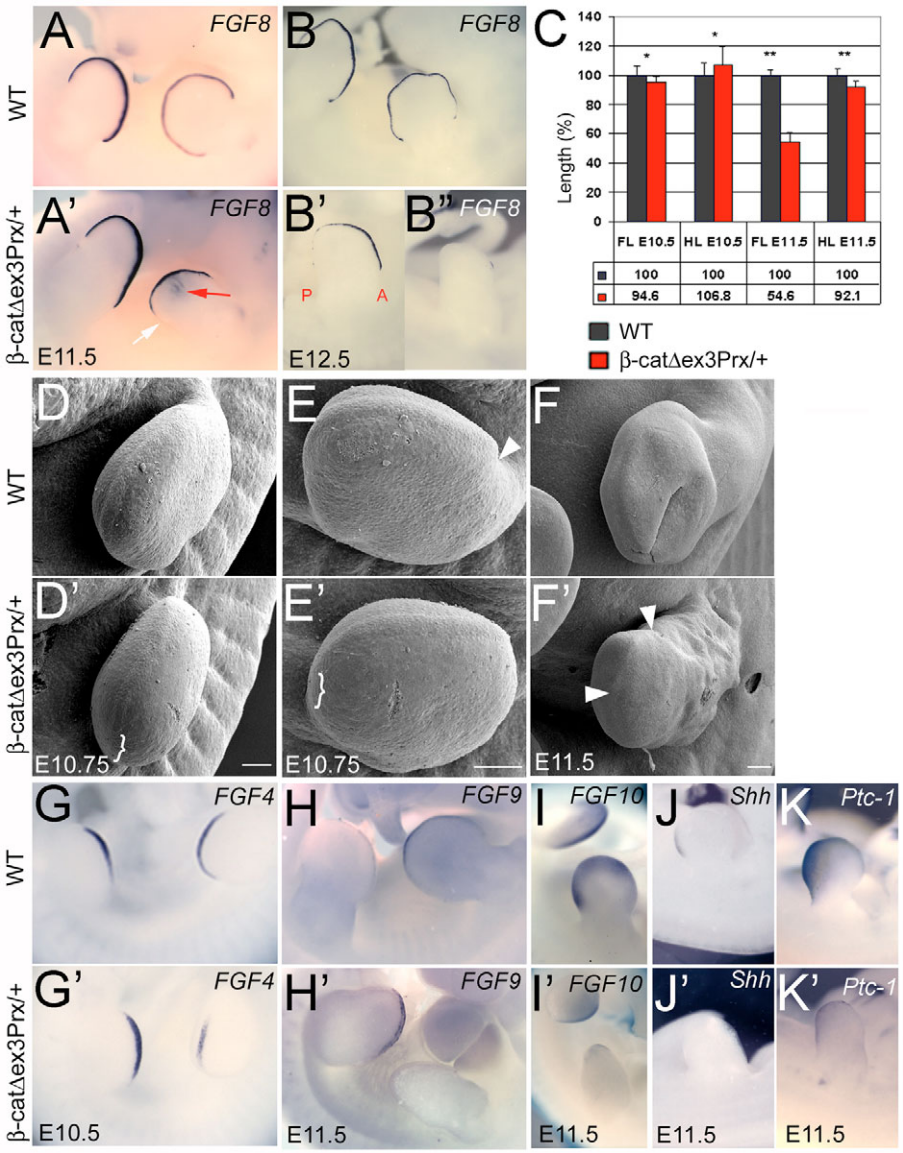

Fig. 3. SEM and marker analysis of embryos with activated Wnt/β-catenin signaling in the limb mesenchyme. (**A**,**A′**) Whole-mount in situ hybridizations showing *Fgf8* expression in wild-type (A) and *β-cat*$^{\Delta ex3Prx1/+}$ (A′, *n*=5) forelimbs at E11.5; note ectopic expression in the distal region (red arrow), as well as the loss from the posterior AER (white arrow). (**B-B″**) *Fgf8* expression at E12.5 in wild-type (B) and *β-cat*$^{\Delta ex3Prx1/+}$ (B′,B″) embryos; note expression is lost from the posterior AER in the hindlimb (B′) and is almost completely lost in the forelimb (B″). (**C**) Comparative quantification of the *Fgf8*-expressing regions (approximating the AER) in fore- and hindlimbs of wild-type and *β-cat*$^{\Delta ex3Prx1/+}$ embryos at E10.5 (WT, *n*=6; *β-cat*$^{\Delta ex3Prx1/+}$, *n*=12; *not significant) and E11.5 (WT, *n*=12; *β-cat*$^{\Delta ex3Prx1/+}$, *n*=6; **significant: forelimb, *P*=0.01, hindlimb, *P*=0.02). (**D-F′**) SEM images of wild-type (D-F) and *β-cat*$^{\Delta ex3Prx1/+}$ (D′-F′) forelimbs at E10.75 and E11.5. Brackets in D′,E′ indicate the flattened region of the AER; arrowhead in E indicates the necrotic region in the wild-type limb; arrowheads in F′ indicate AP extension of the AER. (**G**,**G′**) Wild-type *Fgf4* expression in the posterior AER (G), which is downregulated in *β-cat*$^{\Delta ex3Prx1/+}$ forelimbs (G′). (**H**,**H′**) Wild-type *Fgf9* expression in the AER (H), which is lost in *β-cat*$^{\Delta ex3Prx1/+}$ forelimbs (H′). (**I**,**I′**) Wild-type *Fgf10* expression in the mesenchyme (I), which is lost in *β-cat*$^{\Delta ex3Prx1/+}$ forelimbs (I′). (**J**,**J′**) Wild-type *Shh* expression in the ZPA (J), which is absent in *β-cat*$^{\Delta ex3Prx1/+}$ forelimbs (J′). (**K**,**K′**) Wild-type *Ptc1* expression (K), which is reduced in *β-cat*$^{\Delta ex3Prx1/+}$ forelimbs (K′). Embryos are orientated anterior to the right. P, posterior; A, anterior. Scale bars: 100 μm in D-F′.

the ectopic expression of AER markers. *Fgf8* was expressed ectopically in distal patches in *β-cat*$^{\Delta ex3Prx1/+}$ forelimbs at E10.5 (data not shown) and E11.5 (Fig. 3A′, red arrow). However, this was not observed for other AER markers, such as *Fgf4* (Fig. 3G′, E10.5), *Fgf9* (Fig. 3H′, E11.5) and *Wnt3* (data not shown). *Fgf8* section in situ hybridizations revealed that the ectopic expression was mesenchymal (see Fig. S3B′ in the supplementary material).

In addition to being distally ectopically expressed, *Fgf8* was prematurely lost in *β-cat*$^{\Delta ex3Prx1/+}$ forelimbs from the posterior AER at E11.5 (Fig. 3A′, white arrow). At E12.5, in comparison to wild-type limbs, *Fgf8* expression was either completely absent, or only maintained in the most anterior AER (Fig. 3B″, data not shown), (Fig. 3B). By contrast, although no ectopic *Fgf8* expression was detected in *β-cat*$^{\Delta ex3Prx1/+}$ hindlimbs at E11.5 (Fig. 3A′) or E12.5 (Fig. 3B′), *Fgf8* expression was also lost from the posterior AER from E12.5 onwards (Fig. 3B′). In order to quantify the extent of AER loss, we measured the *Fgf8* expressing region in the fore- and hindlimbs of wild-type and *β-cat*$^{\Delta ex3Prx1/+}$ embryos at E10.5 and E11.5 (Fig. 3C). No significant differences in AER length were detected at E10.5 between wild type and *β-cat*$^{\Delta ex3Prx1/+}$. However, at E11.5 there was a significant reduction in both fore- (45.4%) and hindlimbs (7.9%) of *β-cat*$^{\Delta ex3Prx1/+}$ embryos (Fig. 3C). SEM analyses were performed at E10.75 and E11.5. These revealed slight morphological differences between wild-type (Fig. 3D,E) and *β-cat*$^{\Delta ex3Prx1/+}$ (Fig. 3D′,E′) forelimbs at E10.75, such as a flattened posterior AER (bracket) and differences in the shape (arrowhead). At E11.5, the AER was only visible in the anterior region of *β-cat*$^{\Delta ex3Prx1/+}$ forelimbs (Fig. 3F′, between arrowheads).

As other FGF molecules have been implicated in AER maintenance, we analyzed *Fgf4*, *Fgf9*, *Fgf17* and *Fgf10* expression in *β-cat*$^{\Delta ex3Prx1/+}$ limbs. *Fgf4*, expressed in the posterior AER of wild-type forelimbs up to around E11.5, was severely reduced in the posterior AER of *β-cat*$^{\Delta ex3Prx1/+}$ forelimbs at E10.5 (Fig. 3G′). Similarly, *Fgf9* expression was also prematurely lost in *β-cat*$^{\Delta ex3Prx1/+}$ forelimbs at E11.5 (Fig. 3H,H′). *Fgf17* was already downregulated in the AER of both wild-type and *β-cat*$^{\Delta ex3Prx1/+}$ forelimbs around E10.5 (data not shown). Mesenchymal expression of *Fgf10* was not altered at early stages, but was reduced in *β-cat*$^{\Delta ex3Prx1/+}$ forelimbs from E11 onwards (Fig. 3I,I′; and data not shown). The premature loss of AER markers and *Fgf10* in gain-of-function limbs suggests premature regression of the AER.

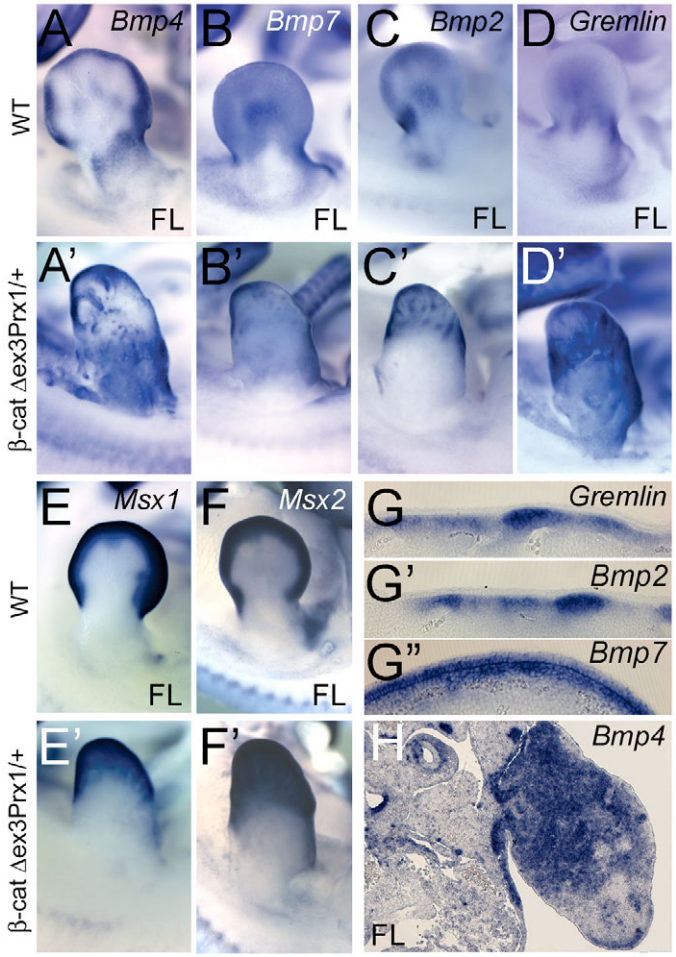

Fig. 4. Upregulation of Bmps and Bmp target genes upon stabilization of β-catenin in limb mesenchyme. (**A-H**) In situ hybridisation showing the expression of Bmps and Bmp target genes in wild-type and *β-cat*$^{\Delta ex3Prx1/+}$ forelimbs at E11.5. (A) Wild-type *Bmp4* expression in the distal mesenchyme and AER. (A′) Expanded *Bmp4* expression in *β-cat*$^{\Delta ex3Prx1/+}$ forelimbs. (B) Wild-type *Bmp7*. (B′) Upregulation of *Bmp7* in *β-cat*$^{\Delta ex3Prx1/+}$. (C) Wild-type *Bmp2*. (C′) Distal upregulation of *Bmp2* in *β-cat*$^{\Delta ex3Prx1/+}$. (D) Wild-type gremlin. (D′) Upregulated gremlin expression in *β-cat*$^{\Delta ex3Prx1/+}$. (E) Wild-type *Msx1*. (E′) Distal upregulation of *Msx1* in *β-cat*$^{\Delta ex3Prx1/+}$. (F) Wild-type *Msx2*. (F′) Upregulation of *Msx2* in distal *β-cat*$^{\Delta ex3Prx1/+}$. (G-G″) Vibratome sections through whole-mount stained *β-cat*$^{\Delta ex3Prx1/+}$ forelimbs demonstrating the mesenchymal upregulation of gremlin (G), *Bmp2* (G′) and *Bmp7* (G″). (H) Section in situ hybridisation for *Bmp4* on E11.5 forelimbs showing upregulation throughout the proximal mesenchyme. Whole-mount stained limbs are orientated anterior to the right and distal up.

AER regression has been linked to a cross-talk between ZPA and AER. Therefore, we analysed the expression of *Shh*, the key ZPA morphogen. *Shh* expression was downregulated in *β-cat*$^{\Delta ex3Prx1/+}$ forelimbs starting at E11.0 (data not shown) and was nearly completely lost at E11.5 (Fig. 3J,J′). Similarly, *Ptc1*, which serves a molecular readout for Shh signaling was highly reduced in E11.5 *β-cat*$^{\Delta ex3Prx1/+}$ limbs (Fig. 3K,K′).

We analyzed whether the levels of Bmps and their target genes were changed in *β-cat*$^{\Delta ex3Prx1/+}$ limbs, as Bmp activity has been implicated in AER regression. At E11.5, *Bmp4* and *Bmp7* were upregulated throughout *β-cat*$^{\Delta ex3Prx1/+}$ fore- and hindlimbs (Fig. 4A′,B′,H, and data not shown), whereas *Bmp2* was only upregulated distally (Fig. 4C′). All three Bmp genes were highly expressed in the most posterior region, including the AER (Fig. 4A′,B′,C′). In addition, the Bmp antagonist gremlin was upregulated (Fig. 4D′), as were the Bmp target genes *Msx1* and *Msx2* in the distal limb (Fig. 4E′,F′). Vibratome sections of whole-mount stained embryos (Fig. 4G-G″), and in situ hybridization on sections (Fig. 4H, and data not shown) demonstrated that the ectopic expression was mesenchymal. Upregulation of Bmp genes and gremlin occurred earlier (E10.5-E10.75) and more extensively in fore- than in hindlimbs (data not shown), implying that the upregulation is probably dependent on the level of activated β-catenin, as Cre recombination occurred earlier in fore- than in hindlimbs. Conversely, levels of *Bmp2*, *Bmp4*, *Bmp7*, gremlin, *Msx1* and *Msx2* were reduced in *β-cat*$^{\Delta Prx1/-}$ limbs at E11.5 (data not shown). Our data suggest that the limb truncations in *β-cat*$^{\Delta ex3Prx1/+}$ embryos are due to a premature regression of the AER, caused by an upregulation of Bmp gene expression and activation of Bmp signaling.

Increased cell death in the mesenchyme of β-catenin mutant limbs

The AER defects observed in β-catenin lof and gof limbs could also be due to excessive cell death in the distal mesenchyme or AER. We therefore performed TUNEL assays on transverse sections through *β-cat*$^{\Delta Prx1/-}$ and *β-cat*$^{\Delta ex3Prx1/+}$ limbs at different developmental stages. At 25 somites, corresponding to the onset of downregulation of *Fgf8* expression, no significant difference in apoptosis was observed (Fig. 5A′). However, more TUNEL-positive cells were detected in the proximal mesenchyme of *β-cat*$^{\Delta Prx1/-}$ forelimbs at E10 (Fig. 5B′). At E11.5, *β-cat*$^{\Delta Prx1/-}$ hindlimbs showed an extensive area of cell death in the central core of the limb bud (data not shown). In gof forelimbs, an increased number of TUNEL-positive cells, predominately scattered throughout the proximal mesenchyme, was detected at E11 (Fig. 5C′). At E11.5, apoptosis had further increased and was more widespread, including distal regions (data not shown). The amount of cell death in the AER was comparable in *β-cat*$^{\Delta ex3Prx1/+}$ and wild-type limbs (Fig. 5C,C′). The temporal occurrence of apoptosis increase in the mesenchyme of gof forelimbs corresponds to Bmp upregulation, suggesting that they may play a role. However, gof hindlimbs, in which Bmps were also expressed ectopically, showed no increase in TUNEL-positive cells at E11.5 (data not shown).

Lmx1b is regulated by β-catenin in the limb mesenchyme

Dorsoventral limb patterning is determined by the correctly localized expression of three genes: *Wnt7a* and *En1*, expressed in dorsal and ventral ectoderm, respectively, and *Lmx1b*, which is regulated by *Wnt7a* and expressed in the dorsal mesenchyme. At E10.5, the ectodermal regulators of *Lmx1b*, *Wnt7a* (Fig. 6A′,A″) and *En1* (Fig. 6B′,B″) were expressed in both *β-catenin* lof and gof limbs similar to wild type (Fig. 6A,B). Loss of β-catenin activity resulted in reduced and partial loss of *Lmx1b* expression in the forelimb already at E9.5 (Fig. 6C′), when compared with wild type (Fig. 6C). Conversely, in β-catenin gof limbs, *Lmx1b* expression was expanded into the ventral mesenchyme at E9.5 (Fig. 6D′, black arrow) compared with wild type (Fig. 6D). At E11.5, *Lmx1b* expression was maintained in *β-cat*$^{\Delta Prx1/-}$ forelimbs, primarily in regions adjacent to the remnants of a functional AER (Fig. 6E′). Section in situ hybridizations on E10.5 *β-cat*$^{\Delta Prx1/-}$ forelimbs revealed an overall downregulation of *Lmx1b* and an even more striking downregulation in the dorsal-most regions, primarily in the

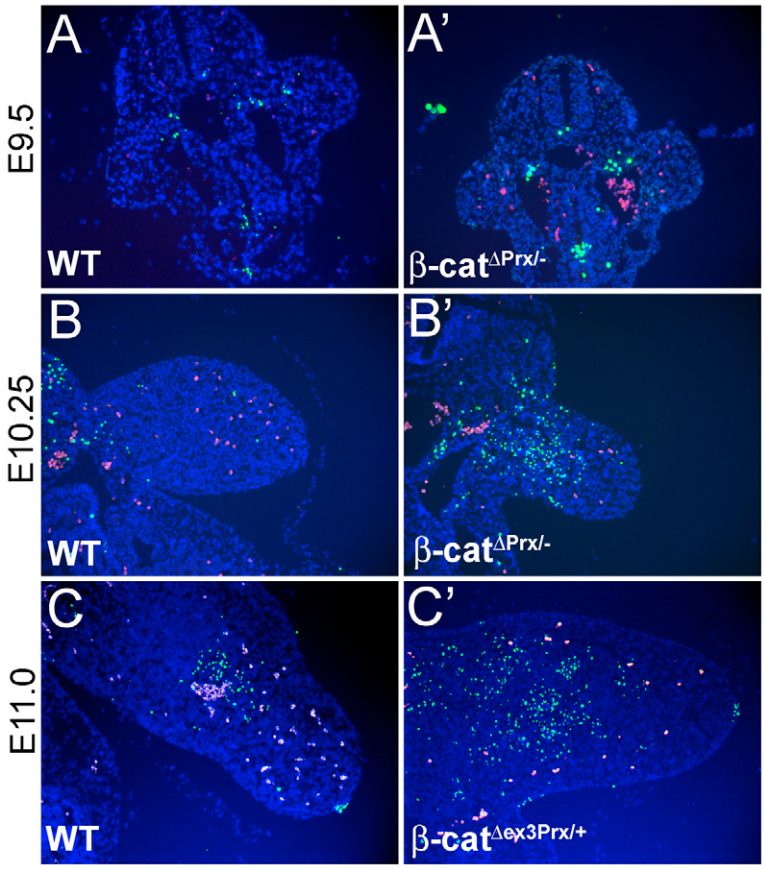

Fig. 5. TUNEL analysis of *β-cat*$^{\Delta Prx1/-}$ and *β-cat*$^{\Delta ex3Prx1/+}$ mutant limb buds. Apoptotic cells are shown in green; red staining indicates autofluorescence. (**A,A′**) E9.5 (25-26 somites) wild-type (A) and *β-cat*$^{\Delta Prx1/-}$ (A′) forelimbs showing no significant apoptosis in the mesenchyme. (**B,B′**) E10.25 forelimbs. A few apoptotic cells are visible in wild type (B), but there is a significant increase in apoptotic cells in the proximal mesenchyme in *β-cat*$^{\Delta Prx1/-}$ (B′). (**C,C′**) E11 forelimb. Apoptosis is detected in the AER and in a central region of the mesenchyme in wild type (C), whereas an increased number of apoptotic cells is observed throughout the proximal mesenchyme in *β-cat*$^{\Delta ex3Prx1/+}$ limbs (C′).

distal half (Fig. 6F′). The expansion of *Lmx1b* into the ventral mesenchyme was clearly visible on E10.5 *β-cat*$^{\Delta ex3Prx1/+}$ forelimb sections. However, a few *Lmx1b*-negative patches were observed within the dorsal and ventral mesenchyme (Fig. 6F″). These areas were not apoptotic, as confirmed by TUNEL staining (data not shown). Notably, no ectopic *Lmx1b* expression directly adjacent to the ventral ectoderm (Fig. 6F″, black arrow) was observed in any of the examined *β-cat*$^{\Delta ex3Prx1/+}$ forelimb sections (n=3). In the hindlimbs, small patches of cells expressing *Lmx1b* adjoining the ventral ectoderm were occasionally detected (n=1/3; data not shown).

The correct localisation of *Wnt7a* and *En1* in the ectoderm of *β-cat*$^{\Delta ex3Prx1/+}$ embryos suggested a cell-autonomous effect on *Lmx1b*. To further investigate this, the distribution of stabilized β-catenin protein was compared with *Lmx1b*, *Lef1* and *Tcf1* expression in *β-cat*$^{\Delta ex3Prx1/+}$ hindlimbs on adjacent sections at E11.5. This revealed high levels of β-catenin protein throughout the entire mesenchyme (black arrow in Fig. 6G′,G″; compared with the trunk, white arrow), intermingled with areas with lower levels (Fig. 6G′,G″; arrowhead). The latter were probably the result of incomplete Cre-recombination. *Lmx1b* expression always correlated with the presence of stabilised β-catenin (Fig. 6G′,H′). However, in the ventral-proximal region, *Lmx1b* was not upregulated, despite the presence of high levels of stabilized β-catenin (Fig. 6G′,H′ black arrows). The two known target genes and transcriptional co-regulators of β-catenin *Lef1* and *Tcf1* (Hovanes et al., 2001; Kengaku et al., 1998) were also upregulated in areas with high levels of β-catenin (Fig. 6I′-J′). In contrast to *Lmx1b*, they were upregulated in ventral-proximal regions (black arrows in Fig. 6I′,J′). Like *Lmx1b*, *Lef1* and *Tcf1* expression were downregulated in β-catenin lof limbs (see Fig. S3D″,E″ in the supplementary material). Double-fluorescent section in situ hybridization revealed that *Lmx1b*-positive cells also upregulated *Lef1* and *Tcf1* (Fig. 6H″,I″,K, and data not shown). Our results suggest that *Lmx1b* is probably regulated, in part, by the canonical Wnt signaling pathway.

β-catenin regulates scapula formation

Early limb patterning defects are often reflected in alterations of internal structures, such as the skeletal elements. Whole-mount Alizarin Red/Alcian Blue skeletal staining of E18.5 embryos revealed the presence of a hypoplastic scapula in the *β-cat*$^{\Delta Prx1/-}$ forelimb. This consisted only of a small remnant of, presumably, the scapula blade (Fig. 7A′, arrowhead) and of a small, round element attached to the proximal end of an element, which is likely to result from incomplete separation of the humerus/radius/ulna anlage (Fig. 7A′, arrow). Section in situ hybridizations on E12.5 forelimbs using probes for collagen 2α1 and *Gdf5* showed that part of the scapula anlage (Fig. 7B, arrowhead) was absent in *β-cat*$^{\Delta Prx1/-}$ embryos (Fig. 7B′, arrowhead). The Gdf5 staining showed that a separate element articulated with the ‘humeral’ end (Fig. 7D′, green arrow). At E14.5, this element (Fig. 7C, black arrow) appeared to be partially fused to the ‘humerus’ (Fig. 7C,E). This element probably corresponds to the glenoid fossa that articulates with the humerus.

As the skeletal elements of loss- and gain-of β-catenin embryos were either severely malformed or almost completely missing, respectively, we analyzed various proximodistal markers, such as *Hoxc6*, *Hoxa9*, *Hoxa10*, *Meis1* and *Meis2*, at E10.5 (Fig. 7F-I″), to see whether limb patterning was still normal (Capdevila et al., 1999; Favier et al., 1996; Fromental-Ramain et al., 1996; Mercader et al., 1999; Nelson et al., 1996; Wahba et al., 2001). The expression of

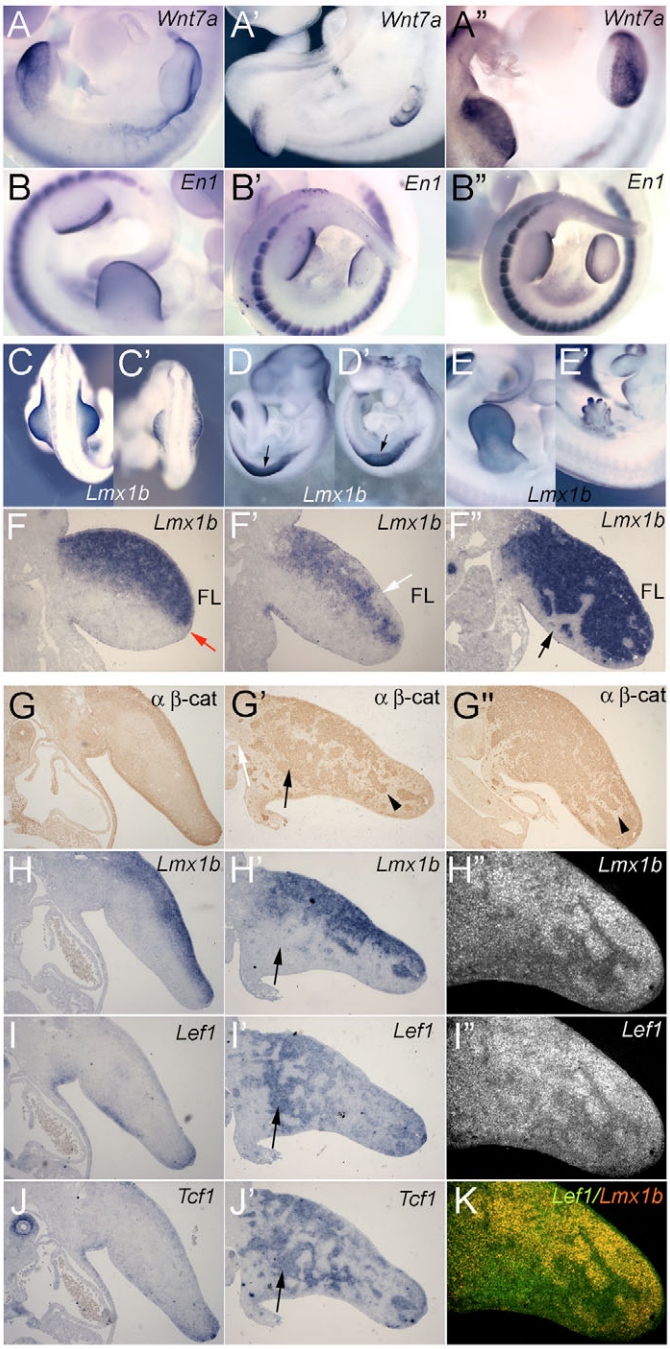

Fig. 6. Regulation of *Lmx1b* expression by β-catenin activity. (**A-B″**) Expression of *Wnt7a* in the dorsal ectoderm (A-A″) and *En1* in the ventral ectoderm (B-B″) at E10.5 in wild-type (A,B), *β-cat*$^{\Delta Prx1/-}$ (A′,B′), and *β-cat*$^{\Delta ex3Prx1/+}$ (A″,B″) fore- and hindlimbs (*n*=4). (**C**,**C′**) Dorsal view of E9.5 embryos showing uniform expression of *Lmx1b* in wild type (C) and downregulation in *β-cat*$^{\Delta Prx1/-}$ (C′, *n*=6) forelimbs. (**D**,**D′**) Lateral view of E9.5 embryos, showing restricted expression of *Lmx1b* in the dorsal mesenchyme (arrow) in wild type (D), which expands into the ventral mesenchyme (arrow) in *β-cat*$^{\Delta ex3Prx1/+}$ (D′) forelimbs. (**E**,**E′**) *Lmx1b* expression at E11.5 in wild-type (E) and *β-cat*$^{\Delta Prx1/-}$ (E′) forelimbs. (**F-K**) Section in situ hybridizations. (F-F″) At E10.5, *Lmx1b* expression is dorsally restricted in wild-type forelimbs (F; delineated by a line running perpendicularly through the AER, red arrow), is reduced and lost in the distal limb mesenchyme adjoining the dorsal ectoderm in *β-cat*$^{\Delta ex3Prx1/+}$ (F′; white arrow), but is expanded into the ventral mesenchyme in *β-cat*$^{\Delta ex3Prx1/+}$ limbs (F″; note, expression is excluded from the ventral-most regions; black arrow; *n*=5). (G-G″) Distribution of β-catenin protein in wild-type (G) and two different E11.5 *β-cat*$^{\Delta ex3Prx1/+}$ (G′,G″) hindlimbs at E11.5. (G-J″) Alternating sections of the same E11.5 wild-type (G-J) and *β-cat*$^{\Delta ex3Prx1/+}$ (G′-J′) hindlimbs. (H,H′) *Lmx1b* expression in wild type (H) and ectopic expression in gof limbs (H′). (I,I′) *Lef1* expression in wild type (I) and ectopic expression in gof limbs (I′). (J,J′) *Tcf1* expression in wild type (J) and ectopic expression in gof limbs (J′). (H″,I″,K) Fluorescent double in situ hybridization on an E11.5 *β-cat*$^{\Delta ex3Prx1/+}$ hindlimb section (same limb as is shown in G″), showing that *Lmx1b*- (H″) and *Lef1* (I″)-positive regions overlap in the distal limb bud (K: *Lef1* green; *Lmx1b* red). Embryos are orientated anterior to the right. Limb bud sections are dorsal up, distal to the right.

Hoxc6, normally expressed in the proximo-anterior region (Fig. 7F), shifted distally in *β-cat*$^{\Delta Prx1/-}$ (Fig. 7F′), but was not altered in *β-cat*$^{\Delta ex3Prx1/+}$ limbs (Fig. 7F″). The Hox genes *Hoxa9* and *Hoxa10*, expressed in the distal regions of the limb (Fig. 7G,H), remained distally expressed in lof (Fig. 7G′,H′) and gof (Fig. 7G″,H″) limbs. The proximal markers *Meis1* and *Meis2* (Fig. 7I, and data not shown) remained proximal in lof (Fig. 7I′) and gof (Fig. 7I″) limbs.

Because the skeletal preparations suggested abnormal scapula development, we analyzed *Pax1* and *Emx2*, two genes that have been shown to be important for scapula formation. Genetic inactivation of *Pax1* results in a specific loss of the acromion, whereas *Emx2* null mice maintain only the glenoid fossa and a small piece of the medio-vertebral border of the scapula (Pellegrini et al., 2001; Timmons et al., 1994; Wilm et al., 1998). In wild type, *Pax1* and *Emx2* were normally expressed in the proximo-anterior forelimb mesenchyme at E10.5 (Fig. 7J,K), whereas their expression was highly reduced in *β-cat*$^{\Delta Prx1/-}$ forelimbs (Fig. 7J′,K′). Section in situ hybridization revealed that *Emx2* was still expressed in a small patch of cells in the anterior-proximal region of *β-cat*$^{\Delta Prx1/-}$ limbs (data not shown).

In *β-cat*$^{\Delta ex3Prx1/+}$ limbs, the *Pax1* domain was slightly reduced (Fig. 7J″), whereas *Emx2* expression was upregulated throughout the proximal limb at E11 (Fig. 7K″). These data suggest that *Emx2*, but not *Pax1*, could be a direct target of canonical Wnt signaling in the developing limb. Furthermore, agenesis of the scapula in lof β-catenin mutants is probably due to the downregulation of *Emx2* and *Pax1* in *β-cat*$^{\Delta Prx1/-}$ mutant embryos.

Stabilizing β-catenin in vitro can upregulate *Emx2* but not *Lmx1b*

Using an in vitro system, we assayed for expression changes of various genes, including *Bmp2*, *Bmp4*, *Bmp7*, *Lmx1b*, *Lef1*, *Tcf1*, *Emx2* and *Twist*, which were upregulated in the *β-cat*$^{\Delta ex3Prx1/+}$ limbs (see Figs 4, 6, 7, and Fig. S3C′,D′,E′ in the supplementary material). Semi-quantitative RT-PCR analysis was performed on RNA from high-density micromass cultures from E11 ex3fl/ex3fl embryos infected with an Adeno-Cre virus, resulting in the accumulation of significant amounts of the N-terminal truncated stabilized form of β-catenin 8-10 hours after transfection (Hill et al., 2005). Control cultures were infected with an Adeno-Gfp virus. *Bmp4*, *Bmp7*, *Lef1*, *Tcf1* and *Emx2* (Fig. 7L, see also Fig. S4 in the supplementary material) were upregulated in this assay, similar to the in vivo observations. Surprisingly, *Lmx1b*, and also *Twist* and *Bmp2*, were not upregulated in vitro, unlike in vivo (Fig. 7L, Figs S3, S4 in the supplementary material). Like in vivo, expression of *Tbx5* and *Fgf10* was not altered (see Fig. S4 in the supplementary material). *Sox9*

was downregulated, as previously shown (Fig. S4 in the supplementary material) (Hill et al., 2005). The in vitro results suggest that *Tcf1*, *Lef1*, *Bmp4*, *Bmp7* and *Emx2* could be direct targets of active β-catenin signaling in the limb. However, *Lmx1b* and also *Twist*, which cannot be upregulated by β-catenin in vitro, might be under the co-regulatory control of a β-catenin-mediated Wnt signal and another signal emanating from the ectoderm in vivo.

DISCUSSION

Requirement for mesenchymal β-catenin for limb outgrowth

Based on studies in chick, it has been proposed that canonical Wnt signaling, together with *Tbx5*, is essential for forelimb initiation and outgrowth (Kawakami et al., 2001; Ng et al., 2002). So far, no Wnt mutant in mouse has been described where limb initiation failed. Similarly, limb initiation still occurs in *Lef1/Tcf1* double mutants; however, this might be due to the presence of *Tcf3* and *Tcf4* (Agarwal et al., 2003). By contrast, inactivation of *Tbx5* activity results in a complete absence of forelimbs or pectoral fins (Agarwal et al., 2003; Ahn et al., 2002; Garrity et al., 2002; Ng et al., 2002; Rallis et al., 2003). Despite the fact that we used the same Cre-deleter line (Prx1-Cre) as in a previous study demonstrating that *Tbx5* is essential for limb initiation (Rallis et al., 2003), we observed limb outgrowth and initially normal expression of *Tbx5*, *Fgf10* and *Fgf8*. This would be in agreement with the previously suggested model that *Tbx5* acts upstream of Wnt/Fgf signaling (Agarwal et al., 2003; Takeuchi et al., 2003). However, the Prx1-Cre line is probably not suitable to address the question of whether canonical Wnt/β-catenin is required for *Tbx5* initiation, as *Tbx5* expression is observed at 8 somites (E8.5) (Agarwal et al., 2003), whereas Prx1-Cre was active only from 15 somites onwards (see Fig. S2 in the supplementary material).

Contrasting with a previous in vitro observation showing that β-catenin can activate a *Fgf10* promoter construct (Agarwal et al., 2003), our results suggest that *Fgf10* is not regulated by Wnt/β-catenin signaling. The observed *Fgf10* downregulation is probably due to a disruption in the *Fgf8/Fgf10*-feedback loop, as *Fgf8* expression in the AER is clearly reduced prior to *Fgf10* expression.

Our data show that mesenchymal β-catenin, together with ectodermal Wnt/β-catenin signaling, is required for *Fgf8* expression and AER maintenance (Barrow et al., 2003; Soshnikova et al., 2003); however, the underlying molecular mechanism needs to be further investigated, as *Fgf10* does not seem to be the direct target. Possible targets could be brachyury or *Twist*, which are regulated by canonical Wnt/β-catenin signaling in other tissues (Galceran et al., 2001; Howe et al., 2003; Yamaguchi et al., 1999b). They are

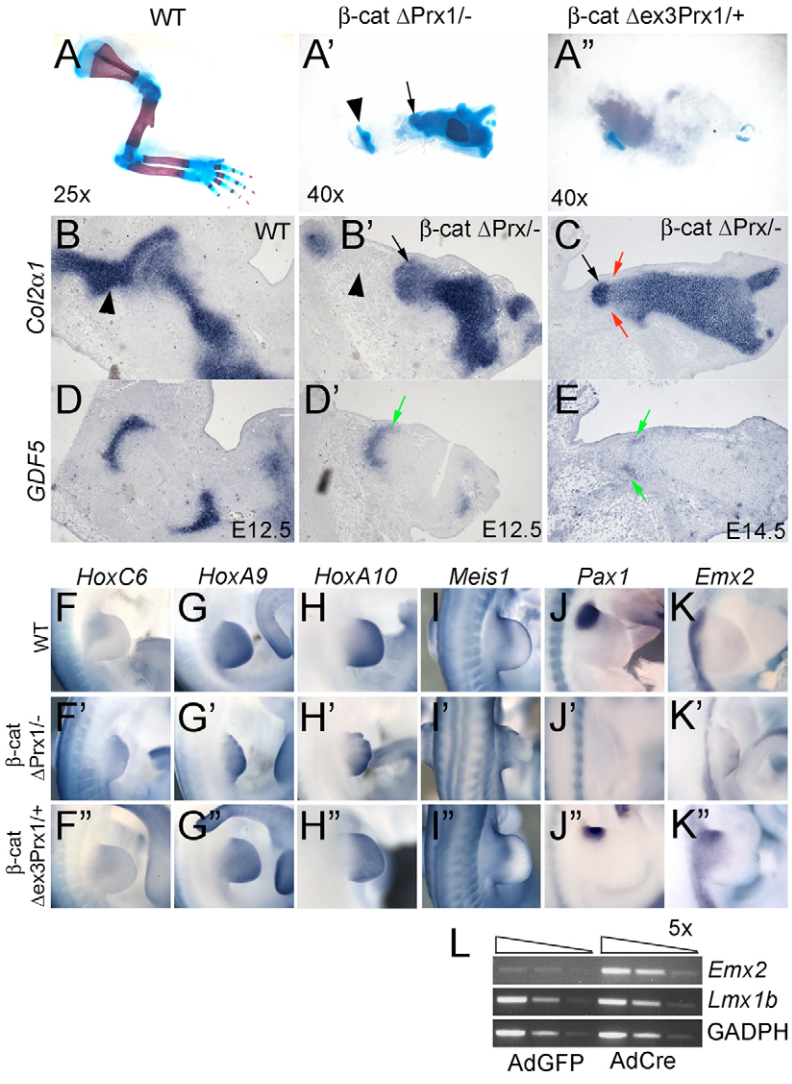

Fig. 7. Shoulder girdle defects in β-catenin loss- and gain-of mutants. (**A-A″**) Alcian Blue/Alizarin Red stained forelimbs from E18.5 wild-type (A), *β-cat*$^{\Delta Prx1/-}$ (A′) and *β-cat*$^{\Delta ex3Prx1/+}$ (A″) embryos (*n*=6), shown at different magnification. (**B-C**) In situ hybridisation for the chondrocyte marker *Col2a1* on E12.5 wild-type (B) and *β-cat*$^{\Delta Prx1/-}$ (B′) and E14.5 *β-cat*$^{\Delta Prx1/-}$ (C) forelimbs, showing partial loss of the scapula anlage (arrowhead in B′) and the presence of a small element (black arrow) separated from the distal element by a zone of low *Col2a1* expression (red arrows, C). (**D-E**) In situ hybridisation for the joint marker *Gdf5* on E12.5 wild-type (D) and *β-cat*$^{\Delta Prx1/-}$ (D′), and E14.5 *β-cat*$^{\Delta Prx1/-}$ (E) forelimbs, showing that *Gdf5* is still expressed (green arrows, D′,E). (**F-K″**) Whole-mount in situ hybridisation for *Hoxc6* (F-F″), *Hoxa9* (G-G″), *Hoxa10* (H-H″), *Meis1* (I-I″), *Pax1* (J-J″) and *Emx2* (K-K″) on E10.5 embryos. *β-cat*$^{\Delta Prx1/-}$ embryos show downregulation of *Pax1* (J′) and *Emx2* (K′; *n*=5). *β-cat*$^{\Delta ex3Prx1/+}$ embryos show reduced *Pax1* (J″) and expanded *Emx2* expression (K″). Embryos are orientated anterior to the top, distal to the right. (**L**) Semi-quantitative RT-PCR from *β-cat ex3fl/ex3fl* Adeno-Cre- and Adeno-GFP (control)-infected micromass cultures showing upregulation of *Emx2* and no upregulation of *Lmx1b* 14 hours after infection.

expressed in the distal mesenchyme and have previously been implicated in AER maintenance (Liu et al., 2003; Zuniga et al., 2002). *Twist* is the most likely candidate, as it was upregulated in gain-, and downregulated in loss-of-function β-catenin limbs (see Fig. 3C′,C″).

Regulation of β-catenin activity in the limb mesenchyme is crucial for the ZPA/AER-feedback loop and the control of AER regression

The proximodistal shortening of *β-cat*$^{\Delta ex3Prx1/+}$ limbs is due to premature regression of the AER starting posteriorly, whereby loss of *Fgf4* and *Fgf9* preceded that of *Fgf8*. Downregulation of *Shh* coincided with the loss of *Fgf4* and *Fgf9*, suggesting that the regression is caused by a disruption in the ZPA/AER-feedback loop (Sun et al., 2000). The molecular mechanism underlying the observed AER regression is probably the β-catenin-mediated upregulation of Bmp genes, as BMPs can induce AER regression (Guha et al., 2002; Khokha et al., 2003; Pizette and Niswander, 1999; Zuniga et al., 1999). This activity is normally antagonized by gremlin (Khokha et al., 2003). Gremlin was also upregulated upon activation of β-catenin; however, we think that this is a secondary effect, because concurrent expansion of the Bmp target genes *Msx1* and *Msx2* suggests that active Bmp signaling was occurring in *β-cat*$^{\Delta ex3Prx1/+}$ limbs, and because Bmps can induce gremlin expression (Pereira et al., 2000).

It is interesting to note that *Wnt5a*, which is expressed in the distal limb mesenchyme, has recently been shown to downregulate β-catenin levels (Topol et al., 2003). *Wnt5a*$^{-/-}$ embryos show a suppression of *Sox9* expression and chondrogenesis in the distal structures, resembling the phenotype of *β-cat*$^{\Delta ex3Prx1/+}$ (Hill et al., 2005; Topol et al., 2003). However, no AER defects have been reported and the expression of Bmp genes was not analyzed in these limbs (Yamaguchi et al., 1999a). These discrepancies could be due to differences in the level or timing of β-catenin stabilization between *β-cat*$^{\Delta ex3Prx1/+}$ and *Wnt5a*$^{-/-}$ embryos. It would certainly be interesting to see which aspects of the *Wnt5a* limb phenotypes could be rescued by removing β-catenin. Proper limb development probably requires the fine-tuning of β-catenin levels in the distal mesenchyme through the *Wnt5a* destabilizing activity and the stabilizing activity of canonical Wnts from the AER.

Lmx1b expression is controlled by β-catenin signaling

Lmx1b expression has been shown to be regulated by *Wnt7a* in chicken and mouse (Cygan et al., 1997; Loomis et al., 1998; Riddle et al., 1995; Vogel et al., 1995); however, it is probably not mediated by the canonical β-catenin pathway (Kengaku et al., 1998). Surprisingly, we found that the loss of β-catenin activity in mice resulted in a downregulation of *Lmx1b* as early as E9.5 in the dorsal mesenchyme. Concomitantly, overactivation of β-catenin resulted in a cell-autonomous upregulation of *Lmx1b*; however, not all regions of the limb were capable of responding. This, together with the observation that *Lmx1b* expression could not be upregulated in vitro, unlike a number of other genes that were also upregulated in vivo, suggests that *Lmx1b* regulation by β-catenin requires an additional signaling input.

Despite the recent data showing that Wnt7a signaling in the presence of Lrp6 stabilizes β-catenin (Adamska et al., 2005; Caricasole et al., 2003), we do not think that *Wnt7a* uses the canonical pathway to regulate *Lmx1b*. Especially because *Lmx1b* expression is only downregulated in the distal mesenchyme of *Wnt7a* and *Lrp6* knockout mice at E11.5 and E12.5, respectively (Adamska et al., 2005; Cygan et al., 1997), whereas in *β-cat*$^{\Delta Prx1/-}$ limbs it is reduced as early as E9.5. *Lmx1b* is also upregulated in *β-cat*$^{\Delta ex3Prx1/+}$ limbs around this stage. By contrast, ectopic *Wnt7a* expression in *En1*$^{-/-}$ limbs from E9.5 onwards leads to ventral expansion of *Lmx1b* only at E11.0 (Cygan et al., 1997; Loomis et al., 1998). Therefore, we favor the hypothesis that, in addition to *Wnt7a*, one or more Wnt(s) are involved in *Lmx1b* regulation, and that these other Wnt(s) signal through the canonical pathway. Possible candidates would be *Wnt3*, *Wnt4*, *Wnt6* and *Wnt7b*, which are expressed in the ectoderm (Bennett et al., 2002). However, these Wnts are expressed throughout the limb bud ectoderm and therefore should activate canonical Wnt/β-catenin signaling in both dorsal and ventral mesenchyme adjacent to the ectoderm. This would correspond to the observed high levels of β-catenin protein, and the expression of *Tcf1* and *Lef1* in the subectodermal mesenchyme (Fig. 6). Therefore, we propose that β-catenin-dependent *Lmx1b* expression requires probably an additional factor, emanating from the dorsal ectoderm or restricted to the dorsal mesenchyme. This is in agreement with the observation that the in vitro stabilization of β-catenin was insufficient to upregulate *Lmx1b*. Alternatively, a secreted repressor of *Lmx1b* may be present in the ventral ectoderm, which could explain why ectopic *Lmx1b* expression was never observed in the ventral-most mesenchyme. Based on our results, we favor a combination of both mechanisms in order to restrict *Lmx1b* to the dorsal mesenchyme. Hence, the ventral ectoderm might play a dual role in preventing *Lmx1b* activation in the ventral mesenchyme: by expressing *En1*, which inhibits *Wnt7a*, and by the expression of a putative secreted inhibitor interfering specifically with β-catenin-mediated activation of *Lmx1b*. Interestingly, loss of β-catenin in the ectoderm also affects dorsoventral patterning, but this is due to loss of *En1* (Barrow et al., 2003; Soshnikova et al., 2003).

β-Catenin is required for scapula development

β-cat$^{\Delta Prx1/-}$ embryos display severe agenesis of the scapula. Although the process of skeletogenesis is closely connected to that of limb patterning, scapula agenesis in mice lacking β-catenin in the limb mesenchyme is probably not caused by the changes observed in skeletal differentiation (Hill et al., 2005). Lack of β-catenin does not inhibit chondrocyte differentiation, on the contrary it stimulates it (Day et al., 2005; Hill et al., 2005). However, in *β-cat*$^{\Delta Prx1/-}$ limbs the cartilaginous scapula anlage is not formed (Fig. 7B′), resembling the *Emx2*$^{-/-}$ phenotype (Pellegrini et al., 2001). Concomitantly, *Emx2*, but also the transcription factor *Pax1*, which is important for scapula formation as well, are severely downregulated (Pellegrini et al., 2001; Timmons et al., 1994; Wilm et al., 1998). The loss of these two transcription factors during early limb bud development is probably the cause for scapula agenesis. β-catenin seems to be necessary and sufficient for *Emx2* expression, making *Emx2* a potential direct target of canonical Wnt/β-catenin signaling in the limb mesenchyme, as has been previously shown in the telencephalon (Backman et al., 2005; Theil et al., 2002). The observed increase in cell death in the proximal region of *β-cat*$^{\Delta Prx1/-}$ limbs at E10 could in principal contribute to scapula agenesis; however, a similar pattern of cell death is observed in *Fgf4*/*Fgf8* double mutants, and even more extensive cell death is found in *Shh* and gremlin mutant limbs, but those develop a normal scapula (Boulet et al., 2004; Michos et al., 2004; Sun et al., 2002; te Welscher et al., 2002).

The loss of the scapula, along with the other appendicular skeletal elements, in *β-cat*$^{\Delta ex3Prx1/+}$ forelimbs is due to the fact that stabilization of β-catenin results in a complete block of

skeletogenesis, as has been shown previously (Hill et al., 2005), and is likely to be independent of the changes in *Emx2* and *Pax1* expression.

Our results provide strong genetic evidence that, in the limb mesenchyme, β-catenin activity is required for AER maintenance, and also, eventually, for its regression, via the control of Bmps. Furthermore, mesenchymal β-catenin signaling is required for dorsal mesenchyme identity through regulation of the dorsal selector gene *Lmx1b*, and, in addition, is required for scapulagenesis, principally via the regulation of *Emx2*.

We thank A. Neubüser, M. Torres, N. G. Copeland, and C. J. Tabin for probes; M. Taschner for technical advice on fluorescent in situ hybridisation; M. Logan for the Prx1-Cre mice; H. Halbritter for SEM assistance; and M. Busslinger and E. Wagner for critical comments. This research was supported by Boehringer Ingelheim.

Supplementary material

Supplementary material for this article is available at http://dev.biologists.org/cgi/content/full/133/7/1219/DC1

References

Adamska, M., Billi, A. C., Cheek, S. and Meisler, M. H. (2005). Genetic interaction between Wnt7a and Lrp6 during patterning of dorsal and posterior structures of the mouse limb. *Dev. Dyn.* **233**, 368-372.

Agarwal, P., Wylie, J. N., Galceran, J., Arkhitko, O., Li, C., Deng, C., Grosschedl, R. and Bruneau, B. G. (2003). Tbx5 is essential for forelimb bud initiation following patterning of the limb field in the mouse embryo. *Development* **130**, 623-633.

Ahn, D. G., Kourakis, M. J., Rohde, L. A., Silver, L. M. and Ho, R. K. (2002). T-box gene tbx5 is essential for formation of the pectoral limb bud. *Nature* **417**, 754-758.

Backman, M., Machon, O., Mygland, L., van den Bout, C. J., Zhong, W., Taketo, M. M. and Krauss, S. (2005). Effects of canonical Wnt signaling on dorso-ventral specification of the mouse telencephalon. *Dev. Biol.* **279**, 155-168.

Barrow, J. R., Thomas, K. R., Boussadia-Zahui, O., Moore, R., Kemler, R., Capecchi, M. R. and McMahon, A. P. (2003). Ectodermal Wnt3/beta-catenin signaling is required for the establishment and maintenance of the apical ectodermal ridge. *Genes Dev.* **17**, 394-409.

Bennett, C. N., Ross, S. E., Longo, K. A., Bajnok, L., Hemati, N., Johnson, K. W., Harrison, S. D. and MacDougald, O. A. (2002). Regulation of Wnt signaling during adipogenesis. *J. Biol. Chem.* **277**, 30998-31004.

Boulet, A. M., Moon, A. M., Arenkiel, B. R. and Capecchi, M. R. (2004). The roles of Fgf4 and Fgf8 in limb bud initiation and outgrowth. *Dev. Biol.* **273**, 361-372.

Capdevila, J., Tsukui, T., Rodriquez Esteban, C., Zappavigna, V. and Izpisua Belmonte, J. C. (1999). Control of vertebrate limb outgrowth by the proximal factor Meis2 and distal antagonism of BMPs by Gremlin. *Mol. Cell* **4**, 839-849.

Caricasole, A., Ferraro, T., Iacovelli, L., Barletta, E., Caruso, A., Melchiorri, D., Terstappen, G. C. and Nicoletti, F. (2003). Functional characterization of WNT7A signaling in PC12 cells: interaction with A FZD5 × LRP6 receptor complex and modulation by Dickkopf proteins. *J. Biol. Chem.* **278**, 37024-37031.

Chen, H., Lun, Y., Ovchinnikov, D., Kokubo, H., Oberg, K. C., Pepicelli, C. V., Gan, L., Lee, B. and Johnson, R. L. (1998). Limb and kidney defects in Lmx1b mutant mice suggest an involvement of LMX1B in human nail patella syndrome. *Nat. Genet.* **19**, 51-55.

Chiang, C., Litingtung, Y., Lee, E., Young, K. E., Corden, J. L., Westphal, H. and Beachy, P. A. (1996). Cyclopia and defective axial patterning in mice lacking Sonic hedgehog gene function. *Nature* **383**, 407-413.

Church, V. L. and Francis-West, P. (2002). Wnt signalling during limb development. *Int. J. Dev. Biol.* **46**, 927-936.

Cygan, J. A., Johnson, R. L. and McMahon, A. P. (1997). Novel regulatory interactions revealed by studies of murine limb pattern in Wnt-7a and En-1 mutants. *Development* **124**, 5021-5032.

Day, T. F., Guo, X., Garrett-Beal, L. and Yang, Y. (2005). Wnt/beta-catenin signaling in mesenchymal progenitors controls osteoblast and chondrocyte differentiation during vertebrate skeletogenesis. *Dev. Cell* **8**, 739-750.

Dreyer, S. D., Zhou, G., Baldini, A., Winterpacht, A., Zabel, B., Cole, W., Johnson, R. L. and Lee, B. (1998). Mutations in LMX1B cause abnormal skeletal patterning and renal dysplasia in nail patella syndrome. *Nat. Genet.* **19**, 47-50.

Favier, B., Rijli, F. M., Fromental-Ramain, C., Fraulob, V., Chambon, P. and Dolle, P. (1996). Functional cooperation between the non-paralogous genes Hoxa-10 and Hoxd-11 in the developing forelimb and axial skeleton. *Development* **122**, 449-460.

Fromental-Ramain, C., Warot, X., Messadecq, N., LeMeur, M., Dolle, P. and Chambon, P. (1996). Hoxa-13 and Hoxd-13 play a crucial role in the patterning of the limb autopod. *Development* **122**, 2997-3011.

Galceran, J., Farinas, I., Depew, M. J., Clevers, H. and Grosschedl, R. (1999). Wnt3a$^{-/-}$-like phenotype and limb deficiency in Lef1(–/–)Tcf1(–/–) mice. *Genes Dev.* **13**, 709-717.

Galceran, J., Hsu, S. C. and Grosschedl, R. (2001). Rescue of a Wnt mutation by an activated form of LEF-1: regulation of maintenance but not initiation of Brachyury expression. *Proc. Natl. Acad. Sci. USA* **98**, 8668-8673.

Garrity, D. M., Childs, S. and Fishman, M. C. (2002). The heartstrings mutation in zebrafish causes heart/fin Tbx5 deficiency syndrome. *Development* **129**, 4635-4645.

Guha, U., Gomes, W. A., Kobayashi, T., Pestell, R. G. and Kessler, J. A. (2002). In vivo evidence that BMP signaling is necessary for apoptosis in the mouse limb. *Dev. Biol.* **249**, 108-120.

Harada, N., Tamai, Y., Ishikawa, T., Sauer, B., Takaku, K., Oshima, M. and Taketo, M. M. (1999). Intestinal polyposis in mice with a dominant stable mutation of the beta-catenin gene. *EMBO J.* **18**, 5931-5942.

Hill, T. P., Spater, D., Taketo, M. M., Birchmeier, W. and Hartmann, C. (2005). Canonical Wnt/beta-catenin signaling prevents osteoblasts from differentiating into chondrocytes. *Dev. Cell* **8**, 727-738.

Hovanes, K., Li, T. W., Munguia, J. E., Truong, T., Milovanovic, T., Lawrence Marsh, J., Holcombe, R. F. and Waterman, M. L. (2001). Beta-catenin-sensitive isoforms of lymphoid enhancer factor-1 are selectively expressed in colon cancer. *Nat. Genet.* **28**, 53-57.

Howe, L. R., Watanabe, O., Leonard, J. and Brown, A. M. (2003). Twist is up-regulated in response to Wnt1 and inhibits mouse mammary cell differentiation. *Cancer Res.* **63**, 1906-1913.

Huelsken, J., Vogel, R., Brinkmann, V., Erdmann, B., Birchmeier, C. and Birchmeier, W. (2000). Requirement for beta-catenin in anterior-posterior axis formation in mice. *J. Cell Biol.* **148**, 567-578.

Huelsken, J., Vogel, R., Erdmann, B., Cotsarelis, G. and Birchmeier, W. (2001). beta-Catenin controls hair follicle morphogenesis and stem cell differentiation in the skin. *Cell* **105**, 533-545.

Kawakami, Y., Capdevila, J., Buscher, D., Itoh, T., Rodriguez Esteban, C. and Izpisua Belmonte, J. C. (2001). WNT signals control FGF-dependent limb initiation and AER induction in the chick embryo. *Cell* **104**, 891-900.

Kengaku, M., Capdevila, J., Rodriguez-Esteban, C., De La Pena, J., Johnson, R. L., Belmonte, J. C. and Tabin, C. J. (1998). Distinct WNT pathways regulating AER formation and dorsoventral polarity in the chick limb bud. *Science* **280**, 1274-1277.

Khokha, M. K., Hsu, D., Brunet, L. J., Dionne, M. S. and Harland, R. M. (2003). Gremlin is the BMP antagonist required for maintenance of Shh and Fgf signals during limb patterning. *Nat. Genet.* **34**, 303-307.

Laufer, E., Nelson, C. E., Johnson, R. L., Morgan, B. A. and Tabin, C. (1994). Sonic hedgehog and Fgf-4 act through a signaling cascade and feedback loop to integrate growth and patterning of the developing limb bud. *Cell* **79**, 993-1003.

Liu, C., Nakamura, E., Knezevic, V., Hunter, S., Thompson, K. and Mackem, S. (2003). A role for the mesenchymal T-box gene Brachyury in AER formation during limb development. *Development* **130**, 1327-1337.

Lobe, C. G. K. K., Kreppner, W., Lomeli, H., Gertsenstein, M. and Nagy, A. (1999). Z/AP, a double reporter for cre-mediated recombination. *Dev. Biol.* **208**, 281-292.

Logan, M., Martin, J. F., Nagy, A., Lobe, C., Olson, E. N. and Tabin, C. J. (2002). Expression of Cre recombinase in the developing mouse limb bud driven by a Prxl enhancer. *Genesis* **33**, 77-80.

Loomis, C. A., Harris, E., Michaud, J., Wurst, W., Hanks, M. and Joyner, A. L. (1996). The mouse Engrailed-1 gene and ventral limb patterning. *Nature* **382**, 360-363.

Loomis, C. A., Kimmel, R. A., Tong, C. X., Michaud, J. and Joyner, A. L. (1998). Analysis of the genetic pathway leading to formation of ectopic apical ectodermal ridges in mouse Engrailed-1 mutant limbs. *Development* **125**, 1137-1148.

Martin, G. R. (1998). The roles of FGFs in the early development of vertebrate limbs. *Genes Dev.* **12**, 1571-1586.

McLeod, M. J. (1980). Differential staining of cartilage and bone in whole mouse fetuses by alcian blue and alizarin red S. *Teratology* **22**, 299-301.

Mercader, N., Leonardo, E., Azpiazu, N., Serrano, A., Morata, G., Martinez, C. and Torres, M. (1999). Conserved regulation of proximodistal limb axis development by Meis1/Hth. *Nature* **402**, 425-429.

Michos, O., Panman, L., Vintersten, K., Beier, K., Zeller, R. and Zuniga, A. (2004). Gremlin-mediated BMP antagonism induces the epithelial-mesenchymal feedback signaling controlling metanephric kidney and limb organogenesis. *Development* **131**, 3401-3410.

Murtaugh, L. C., Chyung, J. H. and Lassar, A. B. (1999). Sonic hedgehog promotes somitic chondrogenesis by altering the cellular response to BMP signaling. *Genes Dev.* **13**, 225-237.

Nelson, C. E., Morgan, B. A., Burke, A. C., Laufer, E., DiMambro, E., Murtaugh, L. C., Gonzales, E., Tessarollo, L., Parada, L. F. and Tabin, C. (1996). Analysis of Hox gene expression in the chick limb bud. *Development* **122**, 1449-1466.

Ng, J. K., Kawakami, Y., Buscher, D., Raya, A., Itoh, T., Koth, C. M., Rodriguez Esteban, C., Rodriguez-Leon, J., Garrity, D. M., Fishman, M. C. et al. (2002). The limb identity gene Tbx5 promotes limb initiation by interacting with Wnt2b and Fgf10. *Development* **129**, 5161-5170.
Niswander, L. (2003). Pattern formation: old models out on a limb. *Nat. Rev. Genet.* **4**, 133-143.
Parr, B. A. and McMahon, A. P. (1995). Dorsalizing signal Wnt-7a required for normal polarity of D-V and A-P axes of mouse limb. *Nature* **374**, 350-353.
Pellegrini, M., Pantano, S., Fumi, M. P., Lucchini, F. and Forabosco, A. (2001). Agenesis of the scapula in Emx2 homozygous mutants. *Dev. Biol.* **232**, 149-156.
Pereira, R. C., Economides, A. N. and Canalis, E. (2000). Bone morphogenetic proteins induce gremlin, a protein that limits their activity in osteoblasts. *Endocrinology* **141**, 4558-4563.
Pizette, S. and Niswander, L. (1999). BMPs negatively regulate structure and function of the limb apical ectodermal ridge. *Development* **126**, 883-894.
Rallis, C., Bruneau, B. G., Del Buono, J., Seidman, C. E., Seidman, J. G., Nissim, S., Tabin, C. J. and Logan, M. P. (2003). Tbx5 is required for forelimb bud formation and continued outgrowth. *Development* **130**, 2741-2751.
Riddle, R. D., Johnson, R. L., Laufer, E. and Tabin, C. (1993). Sonic hedgehog mediates the polarizing activity of the ZPA. *Cell* **75**, 1401-1416.
Riddle, R. D., Ensini, M., Nelson, C., Tsuchida, T., Jessell, T. M. and Tabin, C. (1995). Induction of the LIM homeobox gene Lmx1 by WNT7a establishes dorsoventral pattern in the vertebrate limb. *Cell* **83**, 631-640.
Saunders, J. (1948). The proximo-distal sequence of the origin of the parts of the chick wing and the role of ectoderm. *J. Exp. Zool.* **108**, 363-403.
Scherz, P. J., Harfe, B. D., McMahon, A. P. and Tabin, C. J. (2004). The limb bud Shh-Fgf feedback loop is terminated by expansion of former ZPA cells. *Science* **305**, 396-399.
Soshnikova, N., Zechner, D., Huelsken, J., Mishina, Y., Behringer, R. R., Taketo, M. M., Crenshaw, E. B., 3rd and Birchmeier, W. (2003). Genetic interaction between Wnt/beta-catenin and BMP receptor signaling during formation of the AER and the dorsal-ventral axis in the limb. *Genes Dev.* **17**, 1963-1968.
Sun, X., Lewandoski, M., Meyers, E. N., Liu, Y. H., Maxson, R. E., Jr and Martin, G. R. (2000). Conditional inactivation of Fgf4 reveals complexity of signalling during limb bud development. *Nat. Genet.* **25**, 83-86.
Sun, X., Mariani, F. V. and Martin, G. R. (2002). Functions of FGF signalling from the apical ectodermal ridge in limb development. *Nature* **418**, 501-508.
Takeuchi, J. K., Koshiba-Takeuchi, K., Suzuki, T., Kamimura, M., Ogura, K. and Ogura, T. (2003). Tbx5 and Tbx4 trigger limb initiation through activation of the Wnt/Fgf signaling cascade. *Development* **130**, 2729-2739.
te Welscher, P., Zuniga, A., Kuijper, S., Drenth, T., Goedemans, H. J., Meijlink, F. and Zeller, R. (2002). Progression of vertebrate limb development through SHH-mediated counteraction of GLI3. *Science* **298**, 827-830.
Theil, T., Aydin, S., Koch, S., Grotewold, L. and Ruther, U. (2002). Wnt and Bmp signalling cooperatively regulate graded Emx2 expression in the dorsal telencephalon. *Development* **129**, 3045-3054.
Theiler, K. (1989). *The House Mouse – Atlas of Embryonic Development*. New York, USA: Springer Verlag.
Tickle, C. (2003). Patterning systems – from one end of the limb to the other. *Dev. Cell* **4**, 449-458.
Timmons, P. M., Wallin, J., Rigby, P. W. and Balling, R. (1994). Expression and function of Pax 1 during development of the pectoral girdle. *Development* **120**, 2773-2785.
Topol, L., Jiang, X., Choi, H., Garrett-Beal, L., Carolan, P. J. and Yang, Y. (2003). Wnt-5a inhibits the canonical Wnt pathway by promoting GSK-3-independent beta-catenin degradation. *J. Cell Biol.* **162**, 899-908.
Vogel, A., Rodriguez, C., Warnken, W. and Izpisua Belmonte, J. C. (1995). Dorsal cell fate specified by chick Lmx1 during vertebrate limb development. *Nature* **378**, 716-720.
Wahba, G. M., Hostikka, S. L. and Carpenter, E. M. (2001). The paralogous Hox genes Hoxa10 and Hoxd10 interact to pattern the mouse hindlimb peripheral nervous system and skeleton. *Dev. Biol.* **231**, 87-102.
Wilm, B., Dahl, E., Peters, H., Balling, R. and Imai, K. (1998). Targeted disruption of Pax1 defines its null phenotype and proves haploinsufficiency. *Proc. Natl. Acad. Sci. USA* **95**, 8692-8697.
Yamaguchi, T. P., Bradley, A., McMahon, A. P. and Jones, S. (1999a). A Wnt5a pathway underlies outgrowth of multiple structures in the vertebrate embryo. *Development* **126**, 1211-1223.
Yamaguchi, T. P., Takada, S., Yoshikawa, Y., Wu, N. and McMahon, A. P. (1999b). T (Brachyury) is a direct target of Wnt3a during paraxial mesoderm specification. *Genes Dev.* **13**, 3185-3190.
Yang, Y. (2003). Wnts and wing: Wnt signaling in vertebrate limb development and musculoskeletal morphogenesis. *Birth Defects Res. C Embryo Today* **69**, 305-317.
Zuniga, A., Haramis, A. P., McMahon, A. P. and Zeller, R. (1999). Signal relay by BMP antagonism controls the SHH/FGF4 feedback loop in vertebrate limb buds. *Nature* **401**, 598-602.
Zuniga, A., Quillet, R., Perrin-Schmitt, F. and Zeller, R. (2002). Mouse Twist is required for fibroblast growth factor-mediated epithelial-mesenchymal signalling and cell survival during limb morphogenesis. *Mech. Dev.* **114**, 51-59.
Zuniga, A., Michos, O., Spitz, F., Haramis, A. P., Panman, L., Galli, A., Vintersten, K., Klasen, C., Mansfield, W., Kuc, S. et al. (2004). Mouse limb deformity mutations disrupt a global control region within the large regulatory landscape required for Gremlin expression. *Genes Dev.* **18**, 1553-1564.